Isolation of Cellulose Nanofibers (CNFs) based on Ball-milling Technique Combined with Supercritical Carbon dioxide/ethanol Pretreatment

Zhijun Hu (foxhuz@163.com)
Zhejiang University of Science and Technology https://orcid.org/0000-0003-4530-5871
Xinyu Cao
Zhejiang University of Science and Technology
Guanhong Huang
Zhejiang University of Science and Technology
Daliang Guo
Zhejiang University of Science and Technology

Research Article

Keywords: cellulose nanofibers, ball-milling, supercritical carbon dioxide

Posted Date: March 5th, 2021

DOI: https://doi.org/10.21203/rs.3.rs-277886/v1

Abstract

Here, a new pretreatment method has been developed to produce CNFs from micro-fibrillated cellulose (MFC) by supercritical CO 2 pretreatment followed with ball-milling (SCB). MFC was obtained from cotton stalk by chemical purification.Experimental factors were controlled to enhance the properties of SCB-CNF, meanwhile a comparative study was conducted with the method of TEMPO oxidation and microfluid homogenization (TMH). Compared to TMH-CNF, the SCB-CNF has such advantages as Energy saving, high efficiency and environmental protection, indicating a wide application in heat-resistant materials, load materials and other fields. The solid yields of P-MFC after supercritical CO 2 pretreatment gradually decreased together with the temperature and the reaction time. Scanning electron microscope (SEM) images of the SCB-CNF and TMH-CNF show that the morphology of the SCB-CNF was basically acicular but that of the TMH-CNF was mainly soft fibrous. The SCB-CNF is smaller in width and shorter in length, and its size is between CNC and CNF. Thermal gravimetric results suggest that the thermal stability of the SCB-CNF was substantially higher than those of the TMH-CNF. XRD results indicate that the crystallinity showed an initial increasing trend and then declined with increasing temperature and reaction time, and the crystallinity value of SCB-CNF was larger than that of CNFs. The smaller SCB-CNF became rougher and had a larger surface area. High crystallinity make good thermal stability, short and coarse fiber, easier to disperse than CNF, less energy consumption for dispersion, better than 3D mesh. It can be widely used in polymer composites, reinforcing agents, membrane materials and other fields.

2. Introduction

Cellulose nanofibers (CNFs) from plant biomass are of considerable interest primarily thanks to their high surface area, low density, tunable surface functions, biocompatibility and biodegradability. [1, 2] With these advantages, CNFs have become popular globally in recent years with a great potential in the development of new green nanocomposites [3-4]. CNFs have applications in the engineering field that include and composite materials [5] and biology (drug delivery) [6].

CNFs can be disintegrated from various lignocellulosic sources by separate or in combinated mechanical treatment[7,8] including refining [9], homogenizing [10], micro-fluidization [9-12], grinding, cryocrushing [13-15] and high intensity ultra-sonication [16-18]. Comparing the CNFs produced by homogenization, micro grinding and micro fluidization methods, the CNF produced by homogenization achieved the highest specific surface area. [10] While, CNFs produced by micro grinding and micro fluidization showed superior physical, mechanical and optical properties coupled with reduced energy consumption in comparison with homogenization. Unfortunately, all the above mechanical procedures are energy-intensive which lead to a steep decline in both yields and fibril lengths. Thus, recent studies have shifted the focus to finding high-efficiency, environmentally friendly and low-cost methods to isolate CNF.

Pretreatment before mechanical methods has brought some positive results to the production of CNF[19].

Such as TEMPO oxidation pretreatment. The cellulose nanofibers with uniform width, large aspect ratio, high crystallinity and complete nano dispersion can be prepared by TEMPO catalytic oxidation of cellulose under water medium and normal temperature and pressure. The treatment conditions of TEMPO oxidation system are mild, the raw materials are cheap and relatively environmental friendly. However, there are still some problems in the basic science and practical application of TEMPO pretreatment. For example, when tempo oxidized cellulose is homogenized, the concentration is small and the efficiency is low, which is not conducive to industrial promotion; at present, the construction of high concentration and low viscosity technology of tempo aqueous dispersion solution still needs to be explored by researchers[20].

In recent years, supercritical solvents have been a proposed reaction system with the capability to enhance the effect of the pretreatment process[21]. Supercritical fluids exhibit gas-like diffusivity and liquid-like dissolving capability, which could reduce the heat and mass transfer resistance during the reaction. For example, two-state CO_2 (gaseous and liquid) in the supercritical CO_2 system has higher dissolution capability of polar and non-polar substances, and the liquid CO_2 is acidic and has an autocatalytic effect on water removal from the amorphous region of cellulose. Subcritical water also promotes the hydrolysis of the amorphous and semi-crystalline regions of cellulose. This process shows great potential for cellulose nanocrystal production because it uses only water as the hydrolyzing agent, although it demands additional energy consuming on the use of a high pressurized reactor, the total process is less energy consumption because it does not require high-intensitive mechanical treatment and numerous washing steps. Although, more studies are needed to explore other reaction conditions in order to explain the mechanism of hydrolysis with subcritical water, many successful examples were carried out to improve CNF properties. A combination of pretreatment and refining processes has led to the successful fabrication of uniform CNF with a high degree of fibrillation [22]. Similarly, Wang and Cheng [17] compared the application of high-intensity ultra-sonicationand combination with high-pressure homogenization and found that the combination of the two methods increased the effectiveness of fibrillation and produced uniform nanofibers.

Here, a new pretreatment process has been explored for the preparation of CNF using supercritical carbon dioxide followed by ball milling(SCB). Firstly, the cotton stalk fiber was chemically purified to obtain micro-fibrillated cellulose. Then, Supercritical carbon dioxide/ethanol pretreatment experiments were carried out on cotton stalk micro-fibrillated cellulose (MFC) using a laboratory autoclave. and the yields of pretreated MFC at different temperatures and timeswere examined.

The effect of pretreated conditions on the yields and the mechanism was discussed preliminarily, meanwhile a comparative study was conducted with the method of microfluid homogenization (TMH). The samples were characterized by using X-ray diffraction (XRD), scanning electron microscopy (SEM), Fourier transform infrared spectrometry (FTIR) and thermogravimetric analysis (TGA).

3. Experimental

3.1 Materials

Cotton stalk，Shandong Dongda Cellulose Co. Ltd，and ethanol (99.8%) ，purchased from Aladdin Industrial Co., Hangzhou, China.，

3.2 Preparation of MFC by chemical purification

In order to facilitate the isolation of NCFs from cotton stalk fiber or parenchymal cells, chemical purification, which aims to remove all the non-cellulose polymers from cell walls. A certain amount of cotton stalk material was dewaxed in Soxhlet extractor with 2:1 (v/v) benzyl / ethanol mixture for 6 hours, and then placed in acidified sodium chlorite solution at 75 ℃ for 1 hour to remove lignin from the sample. The lignin removal process was repeated five times until the whole cellulose fiber was obtained and then washed with deionized water. Hemicellulose, residual starch and pectin in the whole cellulose fiber were further removed by 2 wt% KOH at 90 ℃ for 2 hours. Finally, the solution was neutralized with 1 wt% hydrochloric acid, then washed with deionized water and dried.

3.3 Supercritical CO_2/ethanol pretreatment of MFC

A 100-mL high-pressure autoclave (Century Senlong Experimental Apparatus Co. Ltd., Beijing, China) was used for the supercritical CO_2/ethanol pretreatment experiment on MFC. In a typical run, 2.5 g of MFC were placed in the reactor with 75 ml ethanol solution (4:1, v/v). The inside pressure was controlled by injecting carbon dioxide gas (0, 1.5 and 3 Mpa). The reactor was then sealed and allowed to run at a pre-specified temperature of 90 °C -200 °C and a reaction time of 30 min -180 min. The reactor was shock-cooled with water to room temperature as the pretreatment reaction completed. The polymerization products then transferred to a beaker and the reactor was washed by anhydrous ethanol. The mixture of ethanol washing liquid and pretreatment products was filtered through a 0.2-μm microporous filter under vacuum. The retentate (pretreated MFC sample, P-MFC) was vacuum-dried at -30 °C for 24 h to obtain the pretreated MFC product. (see Fig.1- A)

3.4 Methods of preparation of CNFs

Particle size was further reduced by introducing an additional mechanical process using the suspension which was fully reacted with supercritical CO_2 in the ball mill for six hours. There were static and rotating grindstones in the ball-milling equipment and the pulp slurry material passed through these small stones together with the suspension. The goal of fibrillation in the grinder was to ensure the breaking down of the hydrogen bonds and cell wall core structure by shear forces and to reduce the pulp to nano scale fibers [23]. Supercritical CO_2 pretreatment was therefore combined with ball-milling. Mechanical fibrillations by both ball-milling and supercritical CO_2 seemed to randomly dismantle the crystalline and

amorphous regions of the cellulose. This fracture of cellulose crystals is thought to be a factor contributing to the dissociation of micro-fibrils and their bundles [24]. (see Fig.1- A)

The MFC was pretreated by TEMPO oxidation, and then diluted with tap water in a fiber unwinder. The suspension was circulated through a high-pressure homogenizer (tm-lmzo, microfluidics, Westwood, MA) for 20 cycles at 25000 psi to produce TMH-CNFs. (see Fig.1-B)

3.5 Characterization

3.5.1 Yield

$$Yield = \frac{G_1}{G_0} \times 100\% \quad (1)$$

Where, G1 represents the sample after drying and G0 the former MFC (2.5 g). The yield of P-MFC was also used as a response to the experimental design.

3.5.2 Scanning electron microscopy (SEM)

Scanning electron microscopy (SEM) was used for the analysis of the surface morphology of the nano-fibrillated cellulose. Images were captured at a magnification of 10000× by means of a benchtop scanning electron microscope (Ultra55, Carl Zeiss AG, Oberkochen, Germany). The test was operated in high vacuum mode at an acceleration voltage of 15 kV. The samples were secured on a metal stub with carbon and coated with a thin layer of gold using an HR sputter coater (Agar Scientific, Stansted, UK) prior to examination in order to render the products electro-conductive.

3.5.3 XRD

Dried neat CNW films were separately mounted to a special holder through which a beam of x-rays passed through centrally. Scattering radiation was identified in the 2θ range from 2° to 40° at a scanning rate of 4° min^{-1}. The crystallinity index was evaluated from the XRD patterns using equation (2).

$$CI = \frac{I_{200} - I_{am}}{I_{200}} \times 100\% \quad (2)$$

in accordance with the Segal method, where I200 is the intensity height of the crystalline (200) peak (at 2θ = 22.5°), Iam is the minimum intensity height between (200) and (101) peaks (at 2θ = 16.3°)[22].

3.5.4 Fourier transform infrared spectrometry (FT-IR)

The chemical bonds of MFC and P-MFC were analyzed by FT-IR (Nicolet 5700, Thermo-Fisher Scientific, Waltham, MA). The measurement was done using the KBr method for functionality changes in the range 400-4000 cm^{-1} (scans = 32).

3.5.5 Thermal gravimetric analysis

The thermal gravimetric analyzer used in this study was a Pyris Diamond DSC (Perkin Elmer, Waltham, MA). Analysis was conducted in a nitrogen atmosphere, with a nitrogen flow rate of 200 mL min^{-1}. A temperature range of 20 °C -800 °C and a heating rate of 10 °C min^{-1} were used.

4. Results And Discussion

4.1 Effect of carbon dioxide/ethanol pretreatment on the properties of MFC

4.1.1 Yield analysis

The pretreated yields of MFC varied with temperature (120, 135, 150, 180, and 200 °C) and time (30, 90, 120, 150, and 180 min) and are presented in Fig 2. As shown in Fig. 2 (a), when the pretreatment temperature is set at 135 ℃, from 30 min to 150 min the solid-phase yield of p-MFC decreases from 96.1% to 87.3%, which decreases with the prolongation of pretreatment time.

As shown in Fig. 2 (b), when the pretreatment time is set at 90 min, the solid-phase yield of p-MFC reaches the maximum at 135 ℃. Both increasing temperature and lowering temperature will reduce the yield of p-MFC.

When the reaction time was 30 min and the pretreatment temperature was 135 ℃, the solid yields of MFC without supercritical CO_2 pretreatment and with supercritical CO_2 pretreatment were 90.5% and 96.1%, respectively. This indicates that the supercritical CO_2 process may have a definite enhancement effect on the amorphous zone hydrolysis reactions of MFC.

According to the above conclusions, the hydrolysis reaction in amorphous region of MFC increases with the increase of pretreatment temperature and time.

According to Lin & Dufresne [25], the solid yield of p-MFC by supercritical carbon dioxide / ethanol pretreatment process is higher than that of MFC after sulfuric acid pretreatment. It is obvious that the amorphous region of p-MFC is hydrolyzed to a large extent. The higher the yield, the more hydrolysis in the amorphous zone, which proves that sufficient temperature and time can ensure the hydrolysis.

However, with the increase of time and temperature, too severe conditions lead to hydrolysis in the crystallization zone.

4.1.2 SEM analysis

SEM micrographs of MFC pretreated under different conditions are shown in Fig. 3. The surface of MFC was smooth and the single fibers were tightly bonded together. The morphology of P-MFC obtained from MFC pretreated at 135 ºC for 30 min showed that the bunch fiber was divided into a single fiber but the length and diameter of P-MFC were basically maintained (see Fig. 3b). As the pretreatment time increased to 150 min (see Fig 3c), the length and diameter of P-MFC clearly decreased in contrast to P-MFC which did not show a similar trend as the pretreatment temperature increased to 200 °C (see Fig. 3d). The trend in P-MFC morphology suggests that the pretreatment time has a greater effect on the MFC size than the pretreatment temperature. The explanation is that the hydrolysis rate of the reaction at 135 °C was similar to that at 200 °C. A longer reaction time was required to reduce the MFC size by hydrolysis. The supercritical carbon dioxide/ethanol pretreatment can therefore decrease the length and diameter value of MFC under pretreatment conditions of 135 °C for 90 min.

4.1.3 XRD analysis

The XRD patterns of the original MFC material and the P-MFC obtained from MFC pretreatment at different reaction times and temperatures are shown in Figure 4. The diffraction patterns shown by the P-MFC and MFC were similar as shown in Fig. 4, indicating that the hydrolysis by supercritical CO_2 did not alter the crystalline structure of the MFC. All samples showed a sharp peak at 2θ = 23° on the left of the graphs, suggesting that the fibers contained a substantial region of native cellulose I, as shown by the characteristic peak at 22.6°, which corresponds to the lattice plane of cellulose I [26]. This indicates that the hydrolysis by supercritical CO_2 did not change the crystalline structure of the MFC, and this agrees with the results obtained in previous studies[22, 27].

The crystallinity index in Fig. 4 shows that the XRD crystallinity for P-MFC pretreated with supercritical CO_2 increased to 73.98% compared with MFC. The above hypothesis, that the enzyme picked partially digested amorphous regions, is supported by the increase in crystallinity. The crystallinity index of P-MFC initially increased and then decreased as the reaction time increased and this indicates that the amorphous region of MFC hydrolyzed first, and with increasing time the crystalline area was also broken. A reaction time of 90 min may therefore be considered the optimum reaction time in this experiment due to the higher crystallinity index of P-MFC.

Reaction temperature also exerted a substantial effect on the crystallinity of P-MFC. Fig. 4 shows the XRD crystallinity of P-MFC pretreated with supercritical CO_2 at different reaction temperatures. The trend of crystallinity was an initial increase followed by a decline. The amorphous region of the microcrystalline

cellulose hydrolyzed first and with increasing time the crystalline area also hydrolyzed. With supercritical CO_2 pretreatment the crystallinity index of MFC was 78.67% at 135 °C, and this may be regarded as the optimum pretreatment temperature for MFC.

4.1.4 FT-IR analysis

Fig. 5 presents the FT-IR characteristics of the original MFC material and the P-MFC obtained from MFC pretreatment at different reaction times and temperatures. From the diagram the broad absorption band at 3359 cm^{-1} may be attributed to the presence of hydroxyl groups that arise as a result of the association between the polymers. High hydroxyl content is characterized by strong peaking. A more pronounced absorption band can be observed at 3359 cm^{-1} in samples with additional P-MFC, which is associated with the typical O-H vibration of P-MFC. Comparing the different peaks, a stronger characteristic peak indicates a higher functional group content. Additionally, a band at 2900 cm^{-1} was detected showing C-H stretching vibrations, which are due to CH_2 and CH_3 groups. The prominent band at 1043 cm^{-1} was attributed to C-O and C-C stretching and to the contribution of glycosidic linkages.

In Fig. 5 the characteristic peaks at 2915 cm^{-1} correspond to C-H stretching vibration, and this peak vibrates more strongly with increasing temperature. Similarly, the short band at 1662 cm^{-1} in all spectra originates from absorbed moisture. A series of constant short peaks occur during 1043-1440 cm^{-1} which are associated with deformation of C-H bonds on the glucoside keys. In general, the addition of P-MFC did not cause any reactions to generate any new chemical bonds according to the FT-IR curves with 1440 $-CH_2$ bending vibration and 893 C-O-C stretching vibration. This observation is well corroborated with our previous XRD results.

4.2 Comparison on the Characteristics of CNFs

4.2.1 SEM analysis

To determine the size of the SCB-CNF, a dilute suspension was examined using TEM and the images are displayed in Fig. 7. The length of SCB-CNF was about 200-400 nm and the fiber diameter was about 20 nm, while the length of TMH -CNF was about 1-2 μm and the fiber diameter was 20 nm. They bonded together and presented a three-dimensional nano-structured network comprising of randomly arranged nano fibrils. The networks by hydrogen bonds was enabled by the many hydroxyl groups in SCB-CNF. Compared to the MFC materials the surface of the SCB-CNF became rougher, and a trace of erosion by the supercritical CO_2 can be clearly seen. The length and the diameter were almost the same indicated that prolonging the reaction time beyond 90 min did not facilitate the characterization of the SCB-CNF. Meanwhile, the morphology of SCB-CNF is basically acicular, while that of TMH-CNF is mainly soft fibrous. Therefore, SCB-CNF with supercritical CO_2 pretreatment have already had the amorphous region

removed. The pretreatment has an important role in reducing particle size and increasing specific surface area, thereby enhancing thermal stability. The results indicate that this is a potent and environmentally friendly route for the preparation of SCB-CNF.

4.2.2 XRD and FTIR

Comparative XRD in Figs. 4 and 8 show crystalline peaks at 2θ = 14-16°, indicating an increase in the crystallinity of the SCB-CNF and the crystallinity value of SCB-CNF was larger than that of CNFs. It may be concluded that during acid hydrolysis, cellulose possessing a loose structure favors changes in the size of the crystallites. Tang et al. [34] suggested the explanation that changes in crystallite size during acid hydrolysis were a result of both the degradation of smaller crystallites and the growth of the defective crystallites.

Fig. 8 represents the characteristic peaks of SCB-CNF. The broad absorption band at 3395 cm^{-1} is ascribed to hydroxyl groups that arise as a result of the association between the polymers. The characteristic peak was strong, thereby showing that the hydroxyl content was higher. Furthermore, a band at 2248 cm^{-1} was observed and is indicative of C-H stretching vibrations due to CH_2 and CH_3 groups. The prominent band at 1045 cm^{-1} was assigned to C-O and C-C stretching and the glycosidic linkage contribution. A series of constant short peaks occurred from 1045 to 1465 cm^{-1}, and are attributed to the deformation of C-H on the glycoside keys.

Fig. 8 shows the factors related to the reaction time. Compared to Figure 5 there was little change. In general, this indicates that the ball-milling did not generate any new chemical bonds, according to the information on the FT-IR curves .

4.2.3 Thermal gravity

The thermal stability of MFC, P-MFC (135 °C, 1.5 Mpa CO_2, 150 min), and SCB-CNF (135 °C, 1.5 Mpa CO_2, 150 min, ball-milled for 6 h) was determined by thermal gravimetric analysis. Particles exhibited a loss in weight due to increasing temperature and the rate of particle degradation is shown in Fig. 9. An initial weight loss was observed in the MFC (about 350~400 °C) and the SCB-CNF (135 °C, 1.5 Mpa CO_2, 150 min) and is the result of the evaporation of water.

With further increasing temperature (≤ 800 °CC) the TG curves of the MFC and P-MFC (135 °C, 1.5 Mpa CO_2, 150 min) change in a similar fashion. The rate of decomposition and weight loss of the SCB-CNF (135 °C, 1.5 Mpa CO_2, 150 min, ball-milled for 6 h) and the initial degradation temperature of MFC was about 250 °C, lower than the MFC degradation temperature. These results may be explained by saying decreased polymerization and increased specific surface, and consequently the loss of active groups. However, the thermal stability of the SCB-CNF produced by supercritical water hydrolysis was much

higher than that of nano-fibrillated cellulose produced by sulfuric acid hydrolysis owing to the absence of sulfate groups in the SCB-CNF produced by hydrolysis with supercritical CO_2[25]. According to an earlier study[29], the weight loss of SCB-CNF produced by supercritical carbon dioxide is much less than that of nano-fibrillated cellulose produced by sulfuric acid.

The TG curves did not show large changes (≤ 800 °C) with increasing temperature, indicating higher thermal stability. Thus, the thermal stability of the SCB-CNF is clearly higher than those of the TMH-CNF and the raw material. The increased thermal stability of cellulose fibrils (compared to MFC) might be attributed to strong hydrogen bonding between the hydroxyl groups of the cellulose fibrils according to the supercritical carbon dioxide [30]. The higher thermal stability of the SCB-CNF can be attributed to their flexibility and hence a greater possibility of entanglement of the nano fibrils. A comparable increase in thermal stability due to the tangling effect of flexible micro-fibrils has been reported by Das et al. [31]. The melting peaks of the crystalline SCB-CNF were observed in the temperature range 230-250 °C. However, this was not observed in the case of any MFC because the removal of the amorphous portion by chemical treatments in SCB-CNF increased the crystallinity of the SCB-CNF [32].

In most reactions the temperature was the important factor, but the P-MFC yield was predominantly influenced by the timing. According to Fig. 9, carbon dioxide indicates a low significance of the factor. The thermal stability of cellulose whiskers is important, considering their potential application as a reinforcing filler in polymer composites, especially in thermoplastics, as processing temperatures often exceed 200 °C. [32].

5. Conclusions

Here, a novel pretreatment method using supercritical CO_2 was found to be an effective and environmentally friendly reaction medium for cellulose without using an organic solvent. SEM shows that the morphology of SCB-CNF was basically acicular, while that of CNFs was mainly soft fibrous. Thermal gravimetry suggests that the thermal stability of the SCB-CNF was substantially higher than those of the CNFs and the raw material. XRD analysis also indicates that SCB-CNF have higher crystallinity than the MFC or CNFs. The supercritical CO_2 process may have a definite enhancement effect on the amorphous zone hydrolysis reactions of MFC, and hydrolyzed to a greater extent than pretreatment with sulfuric acid, decrease the length and diameter value of MFC under pretreatment conditions of 135 °C for 90 min. The length of SCB-CNF is about 200nm, which is much smaller than that of TMH-CNFpretreated with sulfuric acid.

Declarations

Data Accessibility

Data relating to this work are provided in the electronic supplementary material.

Author Contributions

Z.H. designed the study, carried out the laboratory work and wrote the manuscript. X.C., D.G. and Y.X. carried out the analyses. B.M., P.W., P.C. and J.L. conceived the study, designed the study, coordinated the study and helped draft the manuscript. All authors gave final approval for publication.

Competing interests

We have no competing interest.

Funding Statement

This work was funded by Zhejiang Provincial Key Research and Development Project (No. 2019C01156), Zhejiang Provincial 26 County Green Special project (No. 2019C02042) and Zhejiang Provincial Public Welfare Technology Research Project (No.LGG19C160001),
Zhejiang Philosophy and Social Science Project (No. 20NDJC144YB), the National Natural Science Foundation of China (No. 21808209), and Zhejiang Provincial Natural Science Foundation of China (No. LQ18C160003).

References

1. L. Brinchi, F. Cotana, E. Fortunati, J.M. Kenny, 2013, Production of nanocrystalline cellulose from lignocellulosic biomass: Technology and applications, Carbohydrate Polymers, 94,154-69.
2. N. Durán, A.P. Lemes, M. Durán, J. Freer, J. Baeza, 2011, A minireview of cellulose nanocrystals and its potential integration as co-product in bioethanol production, Journal of the Chilean Chemical Society, 56, 672-677.
3. H.P.S.A. Khalil, A.H. Bhat, A.F.I. Yusra, 2012, Green composites from sustainable cellulose nanofibrils: A review, Carbohydrate Polymers, 87,963-979.
4. J.D. Mendez, C. Weder, Synthesis, 2010, electrical properties, and nanocomposites of poly(3,4-ethylenedioxythiophene) nanorods, Polymer Chemistry, 1,1237-1244.
5. A.C. Leung, S. Hrapovic, E. Lam, Y. Liu, K.B. Male, K.A. Mahmoud, J.H. Luong, 2011, Characteristics and properties of carboxylated cellulose nanocrystals prepared from a novel one-step procedure, Small ,7, 302-5.
6. A.P. Mangalam, J. Simonsen, A.S. Benight, 2009, Cellulose/DNA hybrid nanomaterials, Biomacromolecules, 10,497-504.
7. K.L. Spence, R.A. Venditti, Y. Habibi, O.J. Rojas, J.J. Pawlak, 2010, The effect of chemical composition on microfibrillar cellulose films from wood pulps: Mechanical processing and physical properties, Bioresource Technology, 101, 5961-5968.

8. 18. K.L. Spence, R.A. Venditti, O.J. Rojas, Y. Habibi, J.J. Pawlak, 2011, A comparative study of energy consumption and physical properties of microfibrillated cellulose produced by different processing methods, Cellulose, 18, 1097-1111.
9. W. Stelte, A.R. Sanadi, 2009, Preparation and Characterization of Cellulose Nanofibers from Two Commercial Hardwood and Softwood Pulps, Industrial & Engineering Chemistry Research, 48, 11211-11219.
10. A.N. Nakagaito, H. Yano, 2004, The effect of morphological changes from pulp fiber towards nano-scale fibrillated cellulose on the mechanical properties of high-strength plant fiber based composites, Applied Physics A, 78,547-552.
11. J.Y. Zhu, R. Sabo, X.L. Luo, 2011, Integrated production of nano-fibrillated cellulose and cellulosic biofuel (ethanol) by enzymatic fractionation of wood fibers, Green Chemistry, 13,1339-1344.
12. T. Zimmermann, N. Bordeanu, E. Strub, 2010, Properties of cellulose nanofiber from different raw materials and its reinforcement potential, Carbohydrate Polymers, 79,1086-1093.
13. A. Alemdar, M. Sain. 2008, Isolation and characterization of nanofibers from agricultural residues – Wheat straw and soy hulls, Bioresource Technology, 99,1664-71.
14. A. Chakraborty, M. Sain, M. Kortschot, 2005, Cellulose microfibrils: A novel method of preparation using high shear refining and cryocrushing, Holzforschung, 98,135-107.
15. B. Wang, M. Sain, 2010, Dispersion of soybean stock-based nanofiber in a plastic matrix, Polymer International, 56,538-546.
16. W. Chen, H. Yu, Y. Liu, P. Chen, M. Zhang, Y. Hai, 2011, Individualization of cellulose nanofibers from wood using high-intensity ultrasonication combined with chemical pretreatments, Carbohydrate Polymers, 83, 1804-1811.
17. Q. Cheng, S. Wang, T.G. Rials, 2009, Poly(vinyl alcohol) nanocomposites reinforced with cellulose fibrils isolated by high intensity ultrasonication, Composites Part A, 40,218-224.
18. G.H.D. Tonoli, E.M. Teixeira, A.C. Corrêa, J.M. Marconcini, L.A. Caixeta, M.A. Pereira-Da-Silva, L.H.C. Mattoso, 2012, Cellulose micro/nanofibres from Eucalyptus kraft pulp: Preparation and properties, Carbohydrate Polymers, 89, 80.
19. T. J. Bondancia, L. H. C. Mattoso, José M. Marconcini, & C. S. Farinas. (2017). A new approach to obtain cellulose nanocrystals and ethanol from eucalyptus cellulose pulp via the biochemical pathway. Biotechnology Progress, 33(4).
20. T Saito, S Kimura, Y Nishiyama, et al. 2007, Cellulose nanofibers prepared by TEMPO-mediated oxidation of native cellulose. Biomacromolecules, 8(8), 2485.
21. S. H. Gao 2016, Apocynum bast fiber supercritical CO^2. Collaborative biochemical degumming research [D]. Donghua University.
22. Y. Qing, R. Sabo, J.Y. Zhu, U. Agarwal, Z. Cai, Y. Wu, 2013, A comparative study of cellulose nanofibrils disintegrated via multiple processing approaches, Carbohydrate Polymers, 97, 226-234.

23. I. Siró, D. Plackett, Siro, I. & Plackett, D. 2010, Microfibrillated cellulose and new nanocomposite materials: a review. Cellulose ,17, 459-494, Cellulose, 459-494.
24. X. Wang, Y. Zhang, H. Jiang, Y. Song, Z. Zhou, H. Zhao, 2016, Fabrication and characterization of nano-cellulose aerogels via supercritical CO 2 drying technology, Materials Letters, 183,179-182.
25. N. Lin, A. Dufresne, Surface chemistry, 2014, morphological analysis and properties of cellulose nanocrystals with gradiented sulfation degrees, Nanoscale, 6,5384-93.
26. I. Besbes, S. Alila, S. Boufi, 2011, Cellulose nanofiber from TEMPO-oxidized eucalyptus fibres: Effect of the carboxyl content, Carbohydrate Polymers, 84,975-983.
27. T. Saito, M. Hirota, N. Tamura, S. Kimura, H. Fukuzumi, L. Heux A. Isogai, 2009, Individualization of Nano-Sized Plant Cellulose Fibrils by Direct Surface Carboxylation Using TEMPO Catalyst under Neutral Conditions, Biomacromolecules, 10,1992-6.
28. M. Pääkkö, M. Ankerfors, H. Kosonen, A. Nykänen, S. Ahola, M. Osterberg, J. Ruokolainen, J. Laine, P.T. Larsson, 2007, Enzymatic hydrolysis combined with mechanical shearing and high-pressure homogenization for nanoscale cellulose fibrils and strong gels, Biomacromolecules, 8, 1934-1941.
29. H.D. Jeong, C.R. Yoon, J.H. Lee, D.S. Bang, 2010, Preparation and Characterization of Cellulose Nano-Whiskers Extracted from Microcrystalline Cellulose by Acid Hydrolysis, Toxicon, 45,125–126.
30. G.G. Chen, X.M. Qi, M.P. Li, G. Ying, B. Jing, P. Feng, C.L. Yao, R.C. Sun, 2015, Hemicelluloses/montmorillonite hybrid films with improved mechanical and barrier properties, Scientific Reports, 5, 16405.
31. K. Das, D. Ray, N.R. Bandyopadhyay, S. Sengupta, 2010, Study of the Properties of Microcrystalline Cellulose Particles from Different Renewable Resources by XRD, FTIR, Nanoindentation, TGA and SEM, Journal of Polymers & the Environment, 18, 355-363.
32. K. Das, D. Ray, N.R. Bandyopadhyay, T. Ghosh, A.K. Mohanty, M. Misra, 2009, A study of the mechanical, thermal and morphological properties of microcrystalline cellulose particles prepared from cotton slivers using different acid concentrations, Cellulose, 16, 783-793.
33. W. Gindl, G. Jeronimidis, 2004, Wood pulp fiber reinforced melamine-formaldehyde composites, Journal of Materials Science, 39, 3245-3247.
34. L.G. Tang, N.S. Hon, S.H. Pan, Y.Q. Zhu, Z. Wang,Z.Z. Wang, 1996,Evaluation of microcrystalline cellulose. I. Changes in ultrastructural characteristics during preliminary acid hydrolysis, Journal of Applied Polymer Science, 59, 483-488.

Figures

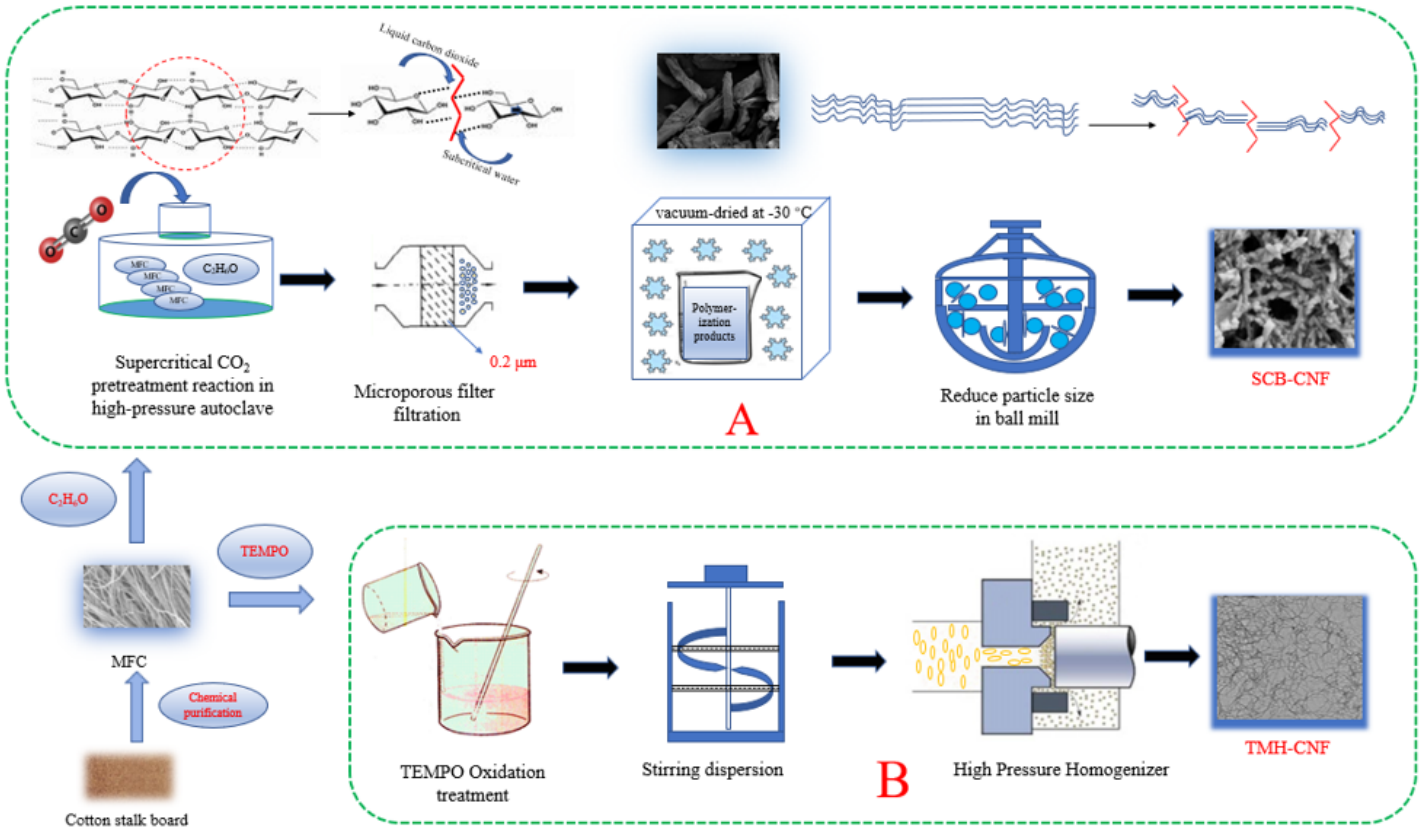

Figure 1

Flow chart of SCB- CNF and TMH-CNF preparation

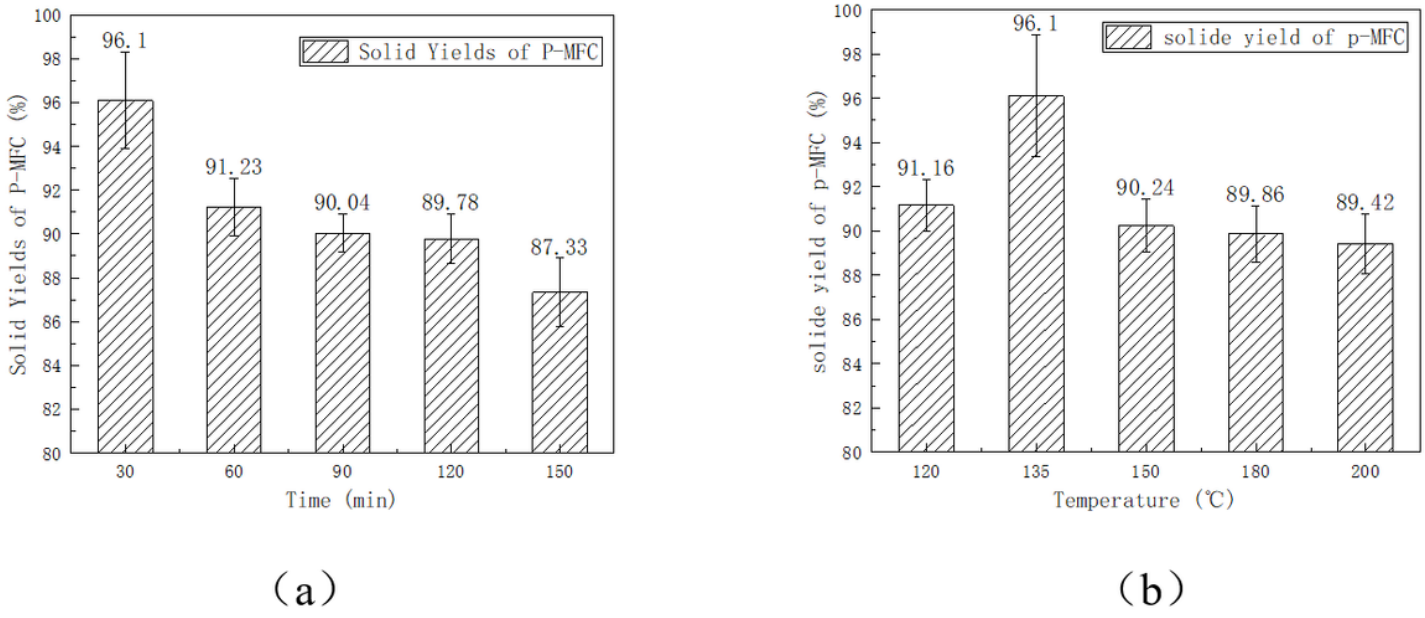

Figure 2

The solid yields of P-MFC with different temperatures and different reaction times

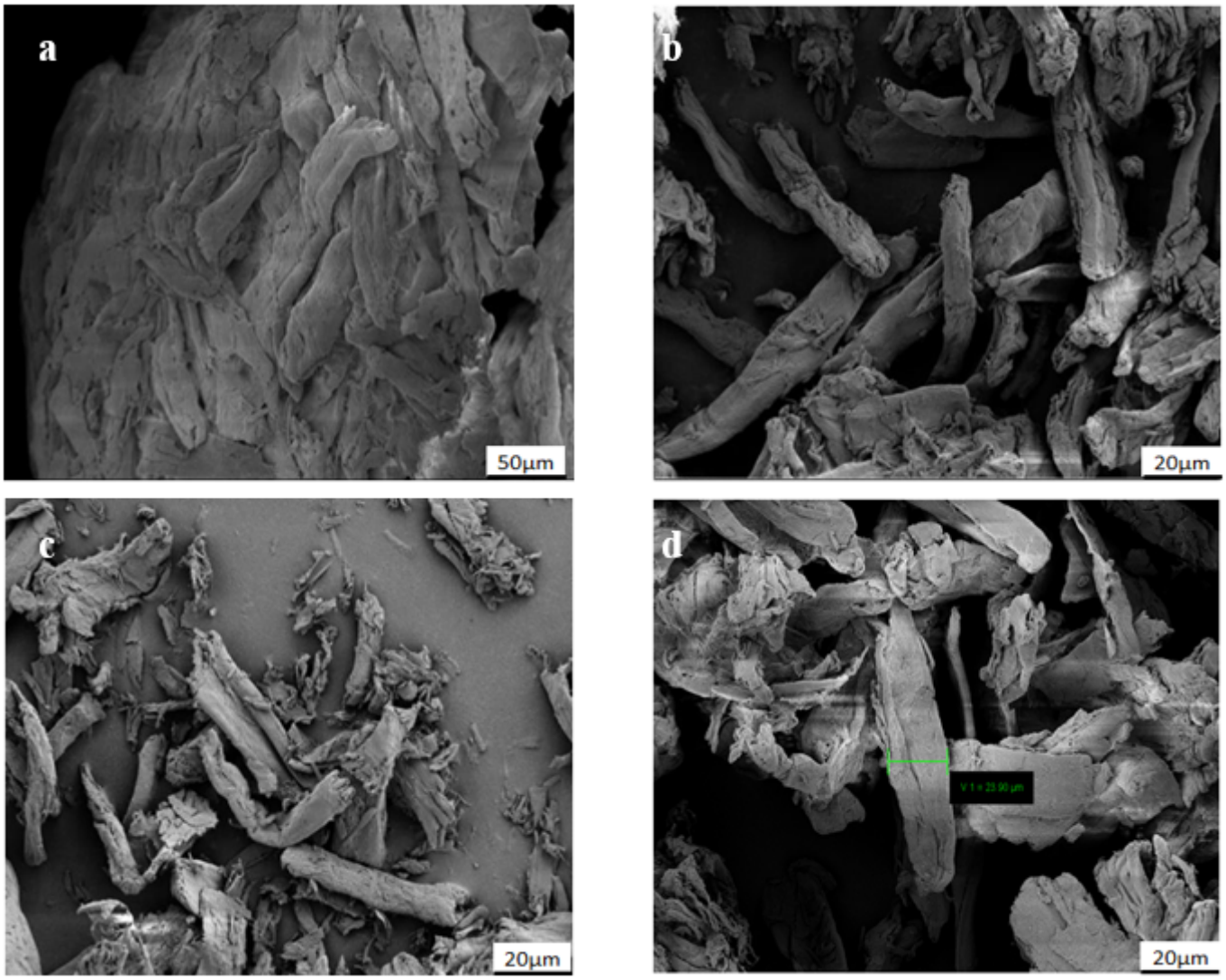

Figure 3

SEM micrographs of P-MFC obtained from MFC pretreated in sub- and super-critical ethanol; (a) MFC; (b) 135 °C, 30min, 1.5Mpa; (c) 135 °C, 150 min, 1.5 Mpa; (d) 200 °C, 30 min, 1.5 Mpa.

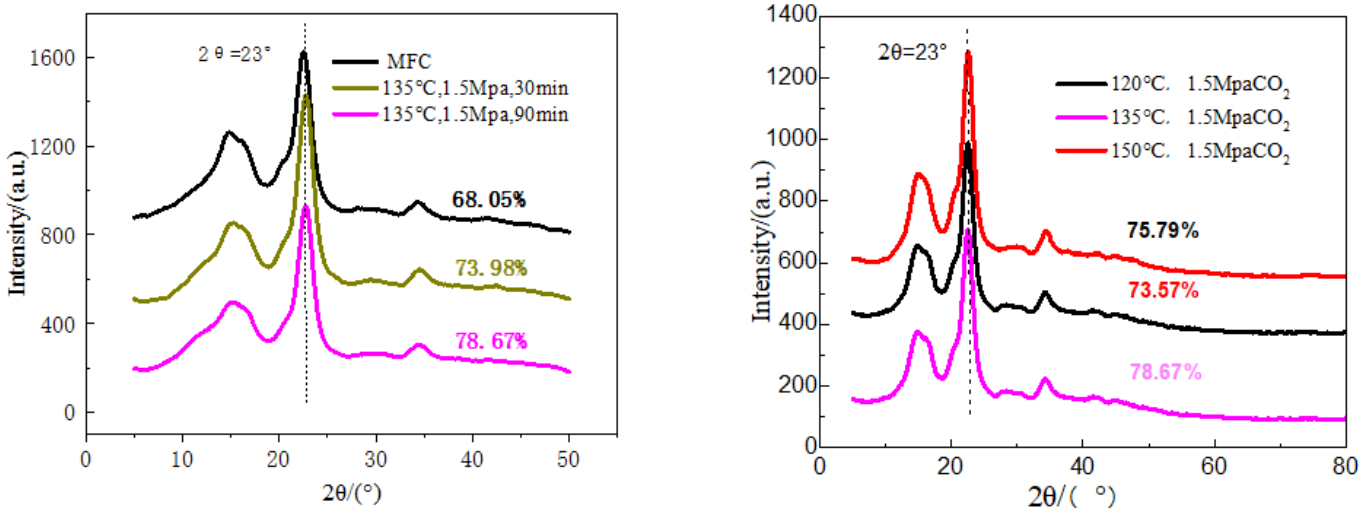

Figure 4

XRD analysis of P-MFC obtained from MFC pretreated for different reaction times and at different reaction temperatures

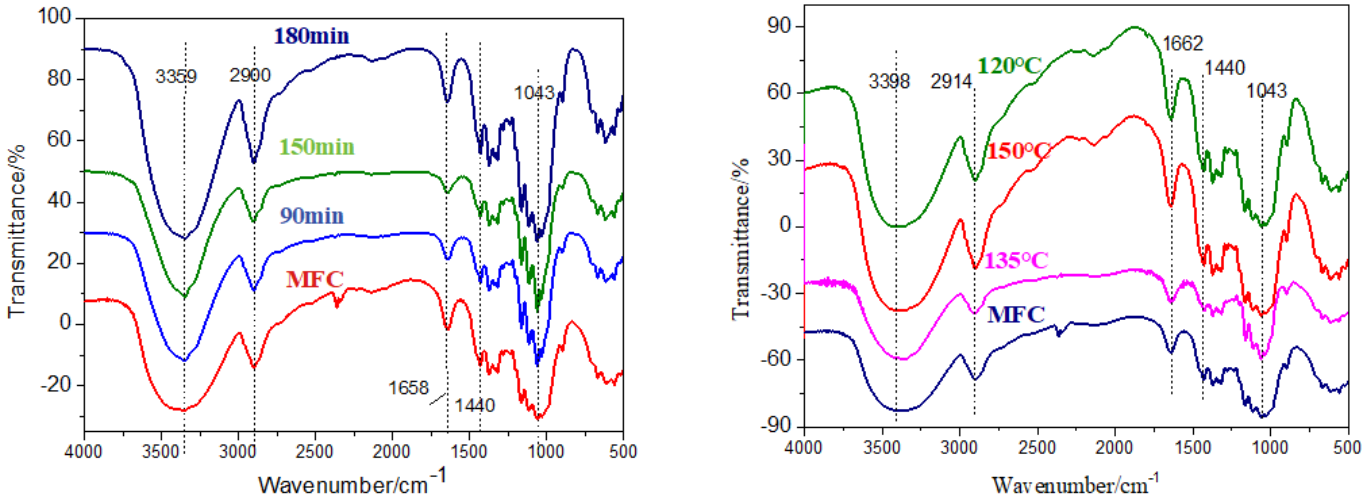

Figure 5

FT-IR analysis of P-MFC obtained from MFC pretreated for different reaction times and at different reaction temperatures

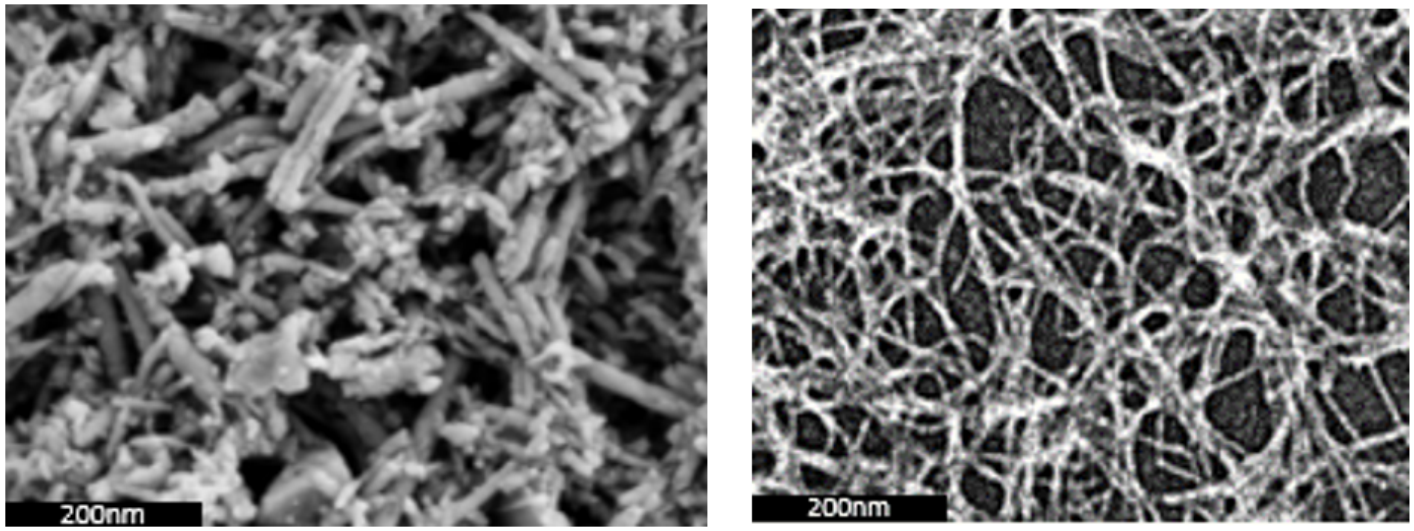

Figure 6

TEM images

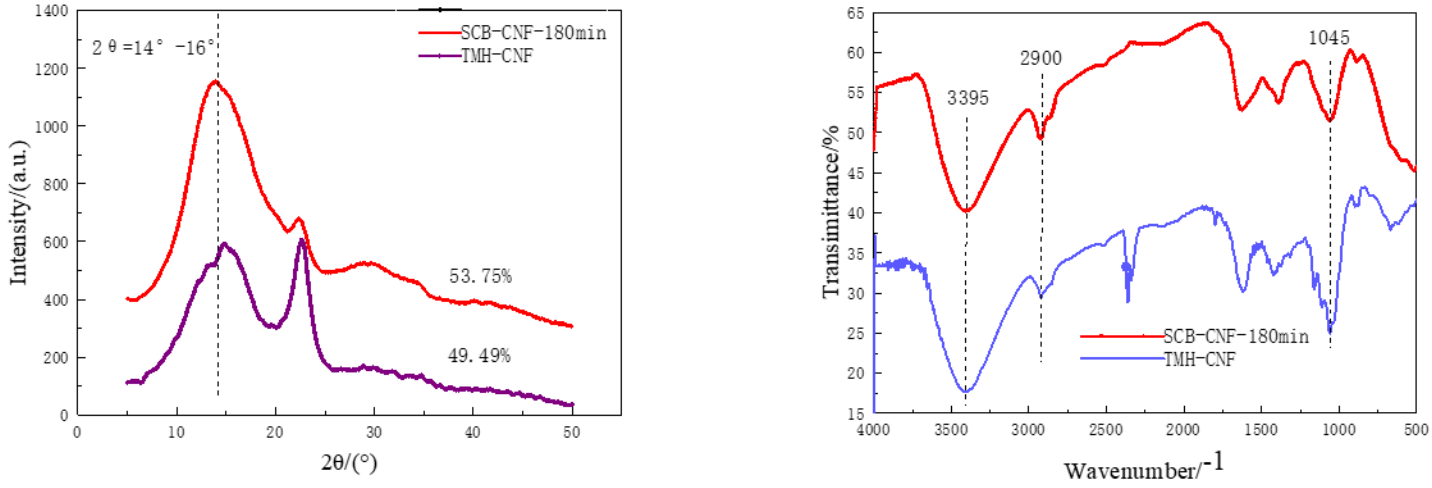

Figure 7

Comparison of XRD and FT-IR of SCB-CNF and TMH-CNF

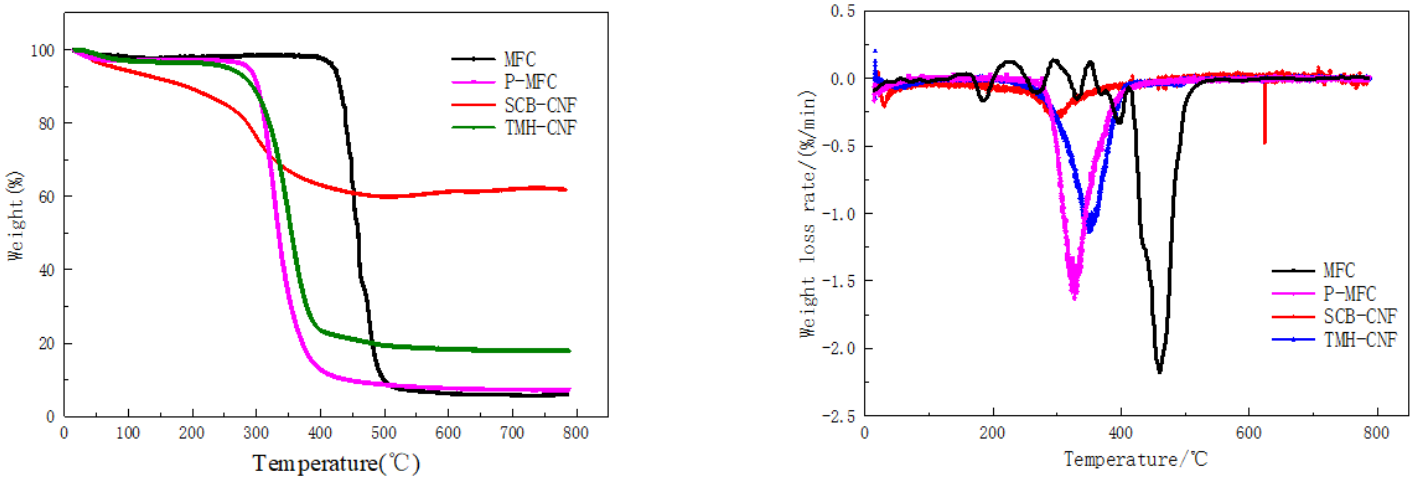

Figure 8

Thermogravimetric analysis of MFC, P-MFC, SCB-CNF and TMH-CNF